Carcinogenesis vol.31 no.7 pp.1230–1237, 2010
doi:10.1093/carcin/bgq097
Advance Access publication May 17, 2010

$G\alpha_{12/13}$ inhibition enhances the anticancer effect of bortezomib through PSMB5 downregulation

Yoon Mee Yang[1], Sanghwan Lee[2], Chang Won Nam[2], Ji Hee Ha[3], Muralidharan Jayaraman[3], Danny N.Dhanasekaran[1,3], Chang Ho Lee[4], Mi-Kyoung Kwak[2] and Sang Geon Kim[1,*]

[1]Department of Pharmacy, College of Pharmacy and Research Institute of Pharmaceutical Sciences, Seoul National University, Seoul 151-742, Korea, [2]Department of Pharmacy, College of Pharmacy, Yeungnam University, 214-1 Dae-dong, Gyeongsan-si, Gyeongsangbuk-do 712-749, Korea, [3]Department of Cell Biology, OU Cancer Institute, The University of Oklahoma Health Sciences Center, Oklahoma City, OK 73104, USA, and [4]Department of Pharmacology and Institute of Biomedical Science, College of Medicine, Hanyang University, Seoul 133-791, Korea

*To whom correspondence should be addressed. Tel: +82 2 880 7840; Fax: +82 2 872 1795;
Email: sgk@snu.ac.kr
Correspondence may also be addressed to Mi-Kyoung Kwak.
Tel: +82 53 810 2823; Fax: +82 53 810 4654;
Email: mkwak@ynu.ac.kr

Bortezomib is a proteasome inhibitor approved for anticancer therapy. However, variable sensitivity of tumor cells exists in this therapy probably due to differences in the expression of proteasome subunits. $G\alpha_{12/13}$ serves modulators or signal transducers in diverse pathways. This study investigated whether cancer cells display differential sensitivity to bortezomib with reference to $G\alpha_{12/13}$ expression, and if so, whether $G\alpha_{12/13}$ affects the expression of proteasome subunits and their activities. Bortezomib treatment exhibited greater sensitivities in Huh7 and SNU886 cells (epithelial type) than SK-Hep1 and SNU449 cells (mesenchymal type) that exhibited higher levels of $G\alpha_{12/13}$. Overexpression of an active mutant of $G\alpha_{12}$ ($G\alpha_{12}$QL) or $G\alpha_{13}$ ($G\alpha_{13}$QL) diminished the ability of bortezomib to induce cytotoxicity in Huh7 cells. Moreover, transfection with the minigene that disturbs G protein-coupled receptor-G protein coupling (CT12 or CT13) increased it in SK-Hep1 cells. Consistently, MiaPaCa2 cells transfected with CT12 or CT13 exhibited a greater sensitivity to bortezomib. Evidence of $G\alpha_{12/13}$'s antagonism on the anticancer effect of bortezomib was verified in the reversal by $G\alpha_{12}$QL or $G\alpha_{13}$QL of the minigenes' enhancement of cytotoxity. Real-time polymerase chain reaction assay enabled us to identify PSMB5, multicatalytic endopeptidase complex-like-1, and proteasome activator subunit-1 repression by CT12 or CT13. Furthermore, $G\alpha_{12/13}$ inhibition enhanced the ability of bortezomib to repress PSMB5, as shown by immunoblotting and proteasome activity assay. Moreover, this inhibitory effect on PSMB5 was attenuated by $G\alpha_{12}$QL or $G\alpha_{13}$QL. In conclusion, the inhibition of $G\alpha_{12/13}$ activities may enhance the anticancer effect of bortezomib through PSMB5 repression, providing insight into the $G\alpha_{12/13}$ pathway for the regulation of proteasomal activity.

Introduction

Targeting protein degradation by inhibiting the ubiquitin–proteasome pathway is a novel approach for cancer therapy. Bortezomib (PS-341, Velcade®) is a dipeptidyl boronic acid that reversibly inhibits the 20S proteasome (1,2). It is a proteasome inhibitor first approved for anticancer therapy, especially for relapsed multiple myeloma and mantle cell lymphoma (i.e. the first-in-class drug). A series of clinical studies of bortezomib have also been conducted in solid tumors. However, the insufficiency of clinical advantage in the studies (3–5) suggests that the targets of bortezomib in solid tumors may not be the same as in hematologic malignancies. Unfortunately, the molecular mechanism associated with this difference is yet unclear.

The 26S proteasome is a multicatalytic proteinase complex containing the 20S core complex in charge of proteolysis and the 19S regulatory complex (6). It may also have a non-proteolytic activity (7). The 20S proteasome consists of a cylindrical stack of rings comprising of the catalytic core subunits β1 (PSMB6), β2 (PSMB7) and β5 (PSMB5). Among the subunits, the chymotrypsin-like activity of PSMB5 seems to be critical for the rate-limiting step of proteolysis (8). Bortezomib primarily targets the chymotrypsin-like activity at PSMB5 (9). However, the expression levels of proteasome subunits, particularly PSMB5, may cause resistance to bortezomib. PSMB5 overexpression or mutation of the gene may account for a resistant mechanism in variants of T-cell lymphoblastic lymphoma or bortezomib-resistant monocytic/macrophages (10–12). In clinical situations, resistance to bortezomib develops in the majority of patients; some even fail to respond to the therapy (13,14).

G protein-coupled receptors (GPCRs) regulate cellular functions through heterotrimeric G proteins consisting of two functional units, a guanine nucleotide binding α-subunit and a βγ-subunit dimer. The α-subunits consist of four families according to their sequence homology (i.e. $G\alpha_s$, $G\alpha_i$, $G\alpha_q$ and $G\alpha_{12}$) (15,16). Among them, the $G\alpha_{12}$ family members ($G\alpha_{12/13}$) have been of particular interest to oncologists since they promote oncogenic transformation and tumor cell growth; $G\alpha_{12/13}$ stimulate anchorage-independent growth (17,18). Moreover, the levels of $G\alpha_{12/13}$ are elevated in patients with breast or prostate cancer, supporting its functional significance in some human cancers (19,20). These G proteins also play a role in cancer invasion and metastasis (e.g. breast, prostate and nasopharyngeal cancers) (19–21).

In view of the importance of $G\alpha_{12/13}$ signals in tumor cell growth, and the lack of an understanding as to the mechanisms of acquired resistance to bortezomib, this study investigated whether epithelial and mesenchymal carcinomas display differential sensitivities to bortezomib in association with the altered $G\alpha_{12/13}$ expression, and if so, whether these G proteins regulate the expression of proteasome subunits and proteasomal activities. Our findings demonstrate that the cytotoxic sensitivity of hepatocellular carcinomas to bortezomib is closely linked to the expression levels of $G\alpha_{12/13}$, implying that these G proteins may enhance resistance of cancer cells to bortezomib. Moreover, this study led to the identification of the ability of the G proteins to induce PSMB5 subunit and consequently increase chymotrypsin-like peptidase activity.

Materials and methods

Materials

Bortezomib was purchased from LC Laboratories (Woburn, MA). *N*-succinyl-Leu-Leu-Val-Tyr-7-amino-4-methylcoumarin (*N*-Suc-LLVY-AMC), Z-Leu-Leu-Glu-7-amino-4-methylcoumarin (Z-LLE-AMC), or Z-Ala-Arg-Arg-7-amino-4-methylcoumarin (Z-ARR-AMC) and MG132 were obtained from Calbiochem (La Jolla, CA). Proteasomal antibodies recognizing PSMB5 were provided from Research Diagnostics (Flanders, NJ). Antibodies directed against active $G\alpha_{13}$ and active Rho were obtained from NewEast Biosciences (Malvern, PA). Antibodies directed against $G\alpha_{12}$, $G\alpha_{13}$ and β-tubulin were supplied from Santa Cruz Biotechnology (Santa Cruz, CA). 3-(4,5-dimethylthiazole-2-yl)-2,5-bdiphenyl tetrazolium bromide (MTT) and dimethyl sulfoxide were purchased from Sigma Chemical (St Louis, MO). DeadEnd™ Colorimetric TUNEL System was provided from Promega (Madison, WI).

Cell culture

Huh7, SNU886, SNU449 and SK-Hep1 cells were obtained from Korean Cell Line Bank (Seoul, Korea). MiaPaCa2 cells were provided from

Abbreviations: DMEM, Dulbecco's modified Eagle's medium; FBS, fetal bovine serum; MECL-1, multicatalytic endopeptidase complex-like-1; mRNA, messenger RNA; MTT, 3-(4,5-dimethylthiazole-2-yl)-2,5-bdiphenyl tetrazolium bromide; PA28α, 11S subunit proteasome activator subunit-1.

Dr D.N. Dhanasekaran. These cell lines were maintained in Dulbecco's modified Eagle's medium (DMEM) (high glucose) supplemented with 10% fetal bovine serum (FBS) and 100 μg/ml Normocin at 37°C in a humidified atmosphere with 5% CO_2. Cells were plated in a six-well dish at a density of 1×10^6 cells per well for 2 days and serum starved for 24 h. Cells were incubated with either bortezomib or MG132 for the time indicated in figure legends.

MTT assay

To measure cytotoxicity, cells were plated in a 48-well dish (1×10^5 cells per well). After drug treatment, viable cells were stained with MTT reagents (0.25 mg/ml) for 4 h. Formazan crystals were dissolved with dimethyl sulfoxide, and absorbance at 540 nm was detected by an enzyme-linked immunosorbent assay microplate reader (Tecan, Research Triangle Park, NC). Cell viability was defined relative to untreated control [i.e. viability (% control) = 100 × (absorbance of treated sample)/(absorbance of control)].

Immunoblot analysis

Immunoblot analyses were performed according to previously published methods (22). Briefly, the cells were lysed in buffer containing 10 mM Tris–HCl (pH 7.1), 100 mM NaCl, 1 mM ethylenediaminetetraacetic acid, 10% glycerol, 0.5% Triton X-100, 0.5% Nonidet P-40, 1 mM dithiothreitol and 0.5 mM phenylmethylsulfonyl fluoride, supplemented with a protease inhibitor cocktail (Calbiochem). Proteins of interest were visualized by the ECL chemiluminescence detection kit (Amersham Biosciences, Buckinghamshire, UK).

Establishment of stably transfected cell lines

Huh7 cells were transfected with pCMV or the plasmid encoding for activated mutant of $G\alpha_{12}$ ($G\alpha_{12}$Q229L and $G\alpha_{12}$QL) or $G\alpha_{13}$ ($G\alpha_{13}$Q226L and $G\alpha_{13}$QL), whereas SK-Hep1 cells were transfected with pcDNA3 or a minigene construct expressing the C-terminal peptide of $G\alpha_{12}$ or $G\alpha_{13}$ (CT12 or CT13) using FuGENE® 6 transfection reagent (Roche Applied Science, Indianapolis, IN). Stable transfectants were selected by incubating the cells in culture medium containing 500 μg/ml Geneticin (G418, Invitrogen, Carlsbad, CA) for Huh7 cells and 1200 μg/ml Geneticin for SK-Hep1 cells for 3 weeks. At least 100 NeoR colonies were pooled together to obtain stably transfected cells. Stable MiaPaCa2 cells were established as described previously (23). Briefly, MiaPaCa2 cells were transfected with pcDNA3 or a minigene construct expressing CT12 or CT13 by electroporation. Transfected cells were splitted in DMEM containing 10% FBS plus 400 μg/ml of active G418. As G418-resistant clones were visible, the concentration of G418 was decreased to 200 μg/ml of active G418. At day 14, the clones were isolated individually. When the cells became confluent, the cells were trypsinized and seeded in 100 mm culture dishes.

TUNEL assay

The DeadEnd™ Colorimetric TUNEL System was used to assay apoptotic cell death, according to the manufacturer's instruction. MiaPaCa2 cells were fixed with 10% buffered formalin in phosphate-buffered saline for 25 min at room temperature. Cells were rinsed with fresh phosphate-buffered saline and then permeabilized with 0.2% Triton X-100 solution in phosphate-buffered saline for 5 min. After equilibrating the cells, each sample was incubated with biotinylated nucleotide mix and terminal deoxynucleotidyltransferase in 100 μl equilibration buffer at 37°C for 1 h. The reaction was terminated by immersing the samples in 2× saline sodium citrate buffer for 15 min. After 0.3% H_2O_2 was added, samples were incubated with 100 μl of horseradish peroxidase-labeled streptavidin solution (1:500). The samples developed using chromogen, H_2O_2 and diaminobenzidine were examined under light microscopy (×200).

Adenoviral infection of $G\alpha_{12}$QL or $G\alpha_{13}$QL

Adenoviruses encoding mouse $G\alpha_{12}$QL (Q229L) was kindly provided from Dr Patrick J. Casey (Duke University Medical Center, Durham, NC). Recombinant adenoviruses were generated by subcloning mouse $G\alpha_{13}$QL (Q226L) into the *attL* containing shuttle plasmid, pENTR-BHRNX (Newgex, Seoul, Korea). Recombinant adenovirus was constructed and generated by using pAd/CMV/V5-DEST gateway plasmid (Invitrogen). Cells were infected at a multiplicity of infection of 50, in DMEM containing 10% FBS for 6 h. Adenovirus which expresses LacZ was used as an infection control.

Real-time polymerase chain reaction assay

Total RNA was extracted using Trizol (Invitrogen) according to the manufacturer's instructions. The complementary DNA was obtained by reverse transcription using an oligo$(dT)_{16}$ primer. It was amplified by polymerase chain reaction. Real-time polymerase chain reaction was conducted with a Light Cycler 1.5 (Roche, Mannheim, Germany) using a Light Cycler DNA master SYBR green-I kit. The following primer sequences were used: human PSMB5, 5′-TGGCTCGGCAATGTCGAATC-3′ and 5′-ACAGATCATGGTGCCCATGG-3′; PSMB6, 5′-TACATCGCCAATCGAGTGAC-3′ and 5′-AGTGGAGGCTCATTCAGTTC-3′; PSMB7, 5′-TGATAACTGCCGCAGGAATG-3′ and 5′-CTTGTCAGCAACAACCATCC-3′; PSMA1, 5′-GCCACAGTTGGTCTGAAATC-3′ and 5′-GAATCCAAACACTCCTGACG-3′; PSMA4, 5′-AAGAAGTGGAGCAGTTGATC-3′and 5′-GCCTTCCTAGTGTGGAAGAG-3′; PSMC4, 5′-GACTTGGAAGACTATGTGGC-3′ and 5′-TGCTCGTCCTTCTTGATGAC-3′; low molecular mass polypeptide 2, 5′-TGCACATCTCATGGTAGCTG-3′ and 5′-AATAGCGTCTGTGGTGAAGC-3′; low molecular mass polypeptide 7, 5′-TCCTGGACTCTACTACGTGG-3′ and 5′-CTCCAGAATAGCTGTCTCTG-3′; multicatalytic endopeptidase complex-like-1 (MECL-1), 5′-ATGTGGACGCATGTGTGATC-3′ and 5′-ATAGCCTGCACAGTTTCCTC-3′; regulatory proteasome non-ATPase subunit 1, 5′-TGGTCAACAAGAGAATAGGC-3′ and 5′-CACTCTGTCGCACAGATCAG-3′; 11S subunit proteasome activator subunit-1 (PA28α), 5′-CTCGGATTGAGGATGGTAAC-3′ and 5′-CACCAGCTGCCGATAATCAC-3′; and hypoxanthine–guanine phosphoribosyltransferase, 5′-TGGCGTCGTGATTAGTGATG-3′ and 5′-GCTACAATGTGATGGCCTCC-3′.

Proteasome activity assay

Proteasome activities were measured in total cell lysates, as described previously (24). Cells were lysed in a buffer containing 50 mM Tris–HCl (pH 7.8), 20 mM KCl, 5 mM $MgCl_2$ and 1 mM dithiothreitol. Fluorogenic peptide (*N*-Suc-LLVY-AMC, Z-LLE-AMC or Z-ARR-AMC, 200 μM) was added into the cell lysates and incubated at 37°C for 20 min. The reaction was terminated by adding an equal volume of 125 mM sodium borate buffer (pH 9.0) consisting of 7.5% ethanol. Released fluorogenic AMC was detected at 368 nm excitation and 467 nm emission wavelengths using a fluorometric plate reader (Molecular Devices).

Data analysis

Scanning densitometry of the immunoblots was performed with the Image Scan and Analysis System (Alpha-Innotech Corporation, San Leandro, CA). One-way analysis of variance procedures were utilized to assess significant differences among treatment groups. For each treatment showing statistically significant effect, the Newman–Keuls test was used to compare multiple group means. The criterion for statistical significance was set at $P < 0.05$ or $P < 0.01$.

Results

The cytotoxic effects of bortezomib on hepatocellular carcinoma cells

To compare the cytotoxic effects of bortezomib on a panel of human hepatocarcinoma cell lines, we first treated Huh7 and SNU886 cells, or SK-Hep1 and SNU449 cells, which were chosen as representative cell lines of epithelial and mesenchymal origins (25), respectively, with increasing concentrations of bortezomib (0.1–10 μM) for 24 h. The growth inhibition of these cells was measured using MTT assay. Intriguingly, the carcinomas of epithelial cell types (Huh7 and SNU886) displayed greater sensitivity to the toxicity of bortezomib than those of mesenchymal cell types (SK-Hep1 and SNU449) (Figure 1A), displaying heterogeneity in the drug responsiveness. As supportive evidence that this differential effect of bortezomib results from proteasomal inhibition, we also evaluated the effect of MG132, another proteasome inhibitor, on the cell viability. Consistently, MG132 treatment inhibited the viability of Huh7 or SNU886 cells in a concentration-dependent manner but failed to do so in SK-Hep1 or SNU449 cells (Figure 1B).

As part of an effort to determine whether this differential sensitivity of hepatocellular carcinomas to bortezomib is associated with the altered levels of $G\alpha_{12/13}$, we next measured the expression of these G proteins. Immunoblot analyses revealed that the expression levels of $G\alpha_{12}$ and $G\alpha_{13}$ were both distinctly greater in SK-Hep1 or SNU449 cells than Huh7 or SNU886 cells (Figure 1C). Our results suggested that the inhibition of proteasome activity by bortezomib may lead to the lesser cytotoxic sensitivity in mesenchymal type of carcinomas than those of epithelial type and which may be associated with the upregulation of $G\alpha_{12/13}$.

The effects of $G\alpha_{12/13}$ activity modulations on bortezomib-induced cytotoxicity

To associate the activation of $G\alpha_{12/13}$ with the decreased anticancer effect of bortezomib, the effect of bortezomib was monitored in Huh7

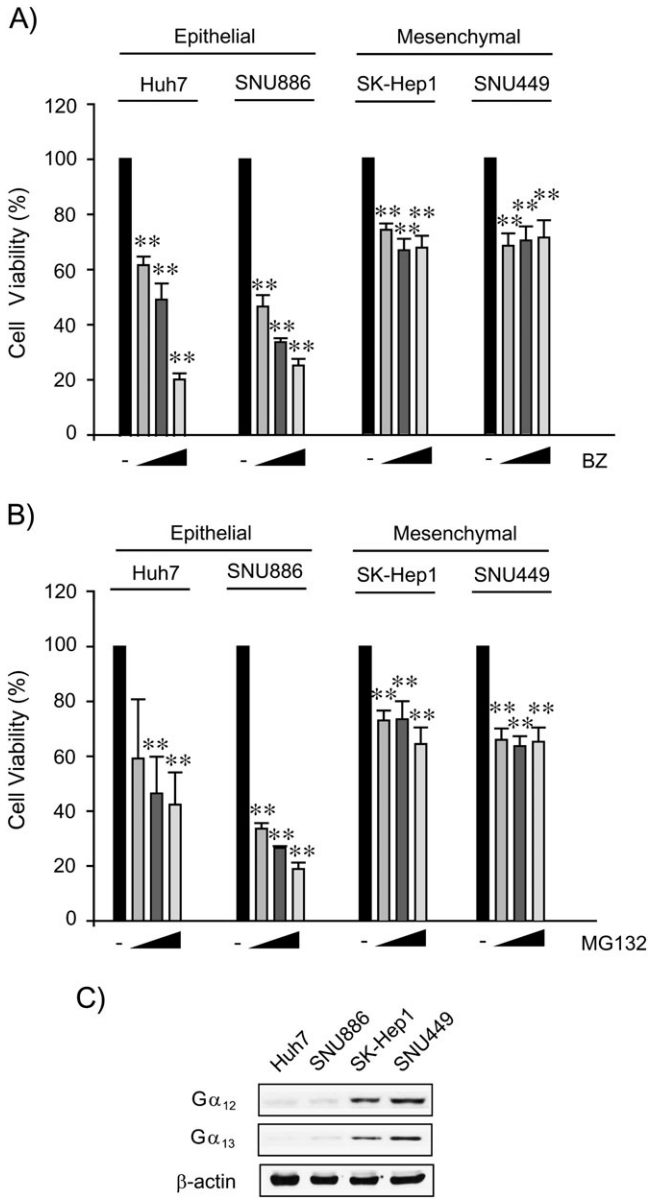

Fig. 1. The cytotoxic effects of bortezomib (BZ) on hepatocellular carcinoma cells. (**A**) Human hepatocellular carcinoma cell lines were treated with 0.1, 1 or 10 μM bortezomib for 24 h following serum starvation (24 h), and their growth inhibition was assessed using MTT assays. (**B**) Viability was also monitored in the cells that had been treated with 0.5, 1 or 5 μM MG132 for 24 h. Values represent the mean ± SE of three independent experiments ($^{**}P < 0.01$, significant compared with untreated control).
(**C**) Immunoblottings for $G\alpha_{12}$ or $G\alpha_{13}$ were performed in the cell lysates. Equal loading of proteins was verified by β-actin. Results were confirmed by three independent experiments.

cells stably transfected with a constitutively active mutant of $G\alpha_{12}$ or $G\alpha_{13}$. Overexpression of a constitutively active mutant of $G\alpha_{12}$ ($G\alpha_{12}$QL) or $G\alpha_{13}$ ($G\alpha_{13}$QL) significantly diminished the ability of bortezomib to induce cytotoxicity in Huh7 cells (Figure 2A). As a continuing effort to link between the expression of $G\alpha_{12/13}$, and altered anticancer activity, the effect of bortezomib treatment on the viability of SK-Hep1 cells was measured after stable transfection of $G\alpha_{12}$ or $G\alpha_{13}$ minigene that disturbs GPCR-$G\alpha_{12/13}$ coupling by C-terminal peptide expression of $G\alpha_{12/13}$ (Figure 2B, lower) (26,27). In this experiment, a decrease in active $G\alpha_{13}$ and/or active Rho verified the appropriate expression of minigenes in these cells (Figure 2B, upper). As expected, minigene inhibition of either $G\alpha_{12}$ or $G\alpha_{13}$ activity rendered this mesenchymal cell type greatly susceptible to bortezomib (Figure 2B, lower).

Given the previous report that MiaPaCa2 cells were extremely resistant to bortezomib with the IC_{50} of >10 μM (28), we were tempted to determine whether the resistance of this cell line resulted from alterations in the activity of $G\alpha_{12/13}$. As expected, the anticancer effect of bortezomib was not observed in MiaPaCa2 cells at the concentrations from 0.1 to 10 μM. However, these cells exhibited sensitivities to bortezomib after transfection with either $G\alpha_{12}$ or $G\alpha_{13}$ minigene (Figure 3A). A similar result was obtained with MG132 treatment. We confirmed the altered cytotoxic effect of bortezomib using TUNEL assay; the number of TUNEL-positive cells was significantly increased in the cells that had been stably transfected with CT12 or CT13 minigene (Figure 3B). As an additional link between $G\alpha_{12/13}$ activity and bortezomib resistance, we assessed the effect of $G\alpha_{12}$QL or $G\alpha_{13}$QL transfection on the cell viability; either transfection of CT12-MiaPaCa2 cells with $G\alpha_{12}$QL or that of CT13-MiaPaCa2 cells with $G\alpha_{13}$QL reversed the sensitivities of these cells to bortezomib (Figure 3C). Collectively, our results that MiaPaCa2 cells exhibited a greater sensitivity to bortezomib after CT12 or CT13 transfection than wild-type cells in conjunction with the reversal by $G\alpha_{12}$QL or $G\alpha_{13}$QL of the minigenes' enhancement of cytotoxic sensitivity demonstrate that $G\alpha_{12/13}$ contribute to the resistance of cancer cells to bortezomib-induced cytotoxicity.

Decreases in the messenger RNA levels of proteasome subunits by CT12 or CT13

To understand more in depth the inhibitory effects of $G\alpha_{12/13}$ on the expression levels of major proteasome subunits, the messenger RNA (mRNA) levels of the catalytic, structural and immunoproteasome subunits of 20S proteasome along with representative subunit genes for 19S and 11S proteasomes were determined in wild-type MiaPaCa2 cells or those transfected with CT12 or CT13. Real-time polymerase chain reaction assay enabled us to identify the significant repression of certain proteasome subunits by CT12, which included PSMB5, MECL-1 and PA28α (Table I). In contrast, inhibition of $G\alpha_{12}$ activity moderately increased the mRNA levels of PSMC4 and 19S component proteasome non-ATPase subunit 1 compared with wild-type control. Moreover, CT13 transfection also repressed PSMB5, PSMB6, MECL-1 and PA28α transcript levels. Inhibition of $G\alpha_{13}$ activity by CT13 also increased the mRNA level of PSMB7. Overall, these results indicate that $G\alpha_{12}$ and $G\alpha_{13}$ may be overlappingly involved in the regulation of PSMB5, MECL-1 and PA28α gene expression. In view of the key role of PSMB5 in the mechanism of cancer cell resistance to bortezomib, we next focused on the regulatory effect of $G\alpha_{12/13}$ on PSMB5 expression.

PSMB5 repression by bortezomib in cells transfected with CT12 or CT13

To address the downstream regulatory effects of $G\alpha_{12/13}$ on PSMB5 expression, we examined time-dependent effects of bortezomib on the PSMB5 transcript levels in wild-type or minigene-transfected MiaPaCa2 cells. In addition to the significant decreases in PSMB5 mRNA by CT12 or CT13 alone, bortezomib treatment further enhanced the ability of CT12 or CT13 to repress PSMB5 mRNA level at 3 h, which was maintained at least up to 12 h posttreatment (Figure 4A). Immunoblottings verified significant decreases in the level of PSMB5 protein in cells transfected with either CT12 or CT13 (Figure 4B). The inhibitory effects of bortezomib on PSMB5 expression could not be assessed by immunoblot assay presumably because of substantial PSMB5 repression by CT12 or CT13 and the low limit of immunoblotting sensitivity.

Next, we assessed the causal relationship between $G\alpha_{12/13}$ activity and PSMB5 expression using $G\alpha_{12}$QL or $G\alpha_{13}$QL. As expected, either $G\alpha_{12}$QL transfection of CT12-MiaPaCa2 cells or $G\alpha_{13}$QL transfection of CT13-MiaPaCa2 cells significantly increased PSMB5 protein levels (Figure 4C). Our results demonstrate that the activation

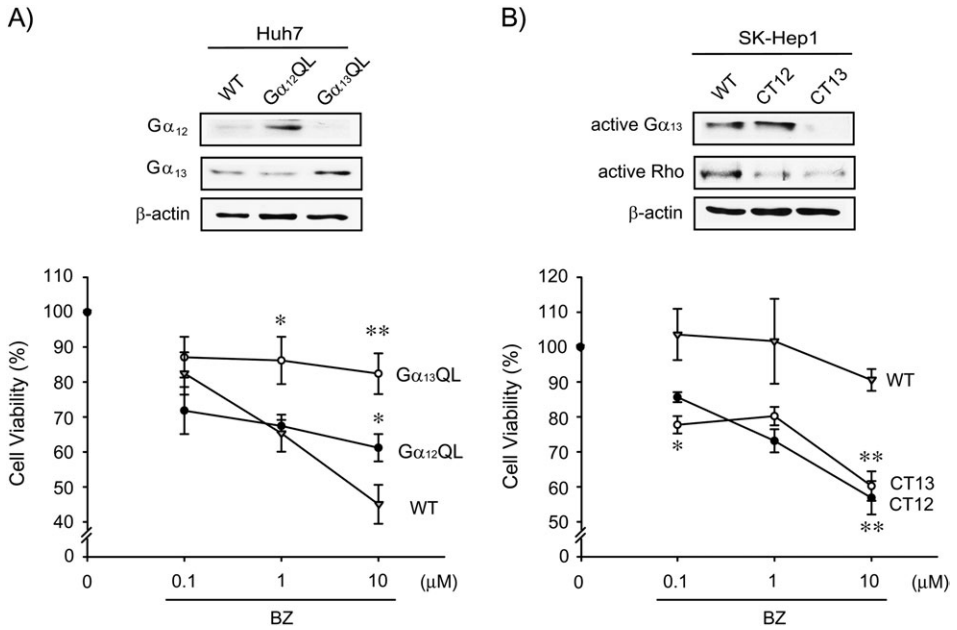

Fig. 2. Changes in the cytotoxic effect of bortezomib (BZ) by $G\alpha_{12}$ or $G\alpha_{13}$ activity modulations. (**A**) The cytotoxicity of bortezomib (10 μM, 24 h treatment) was assessed in Huh7 cells that had been stably transfected with a constitutively active mutant of $G\alpha_{12}$ or $G\alpha_{13}$ ($G\alpha_{12}$QL or $G\alpha_{13}$QL). Data represent the mean ± SE of three independent experiments ($^{*}P < 0.05$, $^{**}P < 0.01$, significant compared with wild-type (WT) cells treated with bortezomib at respective concentrations). Immunoblottings for $G\alpha_{12}$ or $G\alpha_{13}$ verified transfection efficiency. (**B**) The cytotoxicity of bortezomib was measured in SK-Hep1 cells that had been transfected with $G\alpha_{12}$ or $G\alpha_{13}$ minigene (CT12 or CT13). Data represent the mean ± SE of three independent experiments ($^{*}P < 0.05$, $^{**}P < 0.01$, significant compared with wild-type cells treated with bortezomib at respective concentrations). Immunoblottings for active $G\alpha_{13}$ or active Rho confirmed transfection efficiency of the minigenes. Equal loading of proteins was confirmed by immunoblottings for β-actin. Results were confirmed by three independent experiments.

of $G\alpha_{12/13}$ upregulates PSMB5 and that either $G\alpha_{12}$ or $G\alpha_{13}$ inhibition by minigene enhances the ability of bortezomib to repress PSMB5.

Inhibition of proteasome activities by bortezomib in combination with CT12 or CT13

Because CT12 or CT13 not only inhibited the expression of catalytic subunit of 20S proteasome but also did that of PA28α, a 11S proteasome, we finally investigated whether CT12 or CT13 led to inhibition of proteasome activities toward the fluorogenic substrates, *N*-Suc-LLVY-AMC, Z-LLE-AMC and Z-ARR-AMC, which represent chymotrypsin-like, caspase-like and trypsin-like peptidase activities, respectively. Transfection with CT12 resulted in significant decreases in chymotrypsin-like or caspase-like peptidase activities, which were comparable with those accomplished by CT13 transfection (Figure 5). It is also noteworthy that CT13 transfection was more effective in decreasing trypsin-like peptidase activity than CT12 transfection (Figure 5).

Bortezomib primarily targets the chymotrypsin-like activity by inhibiting PSMB5. As expected, we observed that bortezomib effectively inhibited chymotrypsin-like peptidase activity. Moreover, CT12 transfection greatly promoted the ability of bortezomib to inhibit chymotrypsin-like peptidase activity but that of CT13 only marginally increased it. Since bortezomib efficaciously inhibited the caspase-like peptidase activity, additional effect of CT12 or CT13 on the inhibition was minimal. In addition, bortezomib caused no significant change in inhibiting trypsin-like peptidase activity in minigene-transfected cells compared with wild-type ones. Overall, our results demonstrate that the inhibition of $G\alpha_{12}$ or $G\alpha_{13}$ resulted in the repression of proteasome activities in cancer cells resistant to bortezomib.

Discussion

The clinical results of bortezomib therapy in patients with solid malignancies are insufficient for its introduction into clinical practice (29). So, further studies are necessary to reach a clearer understanding of the relevance of bortezomib in the therapy of solid tumors. In particular, hepatocellular carcinoma is ranked the fifth most common cancer worldwide and is a highly malignant tumor that displays resistance to conventional cytostatic agents (30,31). Despite improvement in surgical techniques and operative management, the long-term outcome is unsatisfactory. Hence, advanced disease stages urgently require alternative treatment strategies that focus on targeting pathways in tumor development and maintenance (32). One potential target is the turnover of proteins; certain cancers are exquisitely prone to undergo apoptosis by inhibiting the ubiquitin–proteasome pathway (1).

Targeting the ubiquitin–proteasome pathway by inhibiting the catalytic site of the 26S proteasome is a novel approach for cancer therapy. Bortezomib inhibits chymotrypsin-like activity in proteasome, a rate-limiting step in the proteolysis of intracellular ubiquitinated proteins. Preclinical data have proved useful in identifying several of the biological processes implicated in the action of bortezomib, including cell cycle arrest at the G_2/M phase, cyclin B1 accumulation, increased CDC2/cyclin-dependent kinase 1 activity, p21 upregulation, apoptosis regulation and microvessel density reduction (33,34). The effect of bortezomib on cell cycle arrest may also be due to a non-proteolytic activity (35). The non-proteolytic proteasomal activity unperturbed after bortezomib therapy may affect the equilibrium of the proteasome action, explaining in part an indirect or side effect of bortezomib.

In a phase III trial, it exhibited an antitumor effect in relapsed multiple myeloma patients (36); response rate, time to progression and overall survival were improved in patients treated with bortezomib plus dexamethasone. However, resistance to bortezomib may be a major challenge. A phase II trial in patients with refractory relapsed multiple myeloma demonstrated 35% responses (37); however, a large fraction of patients (i.e. 65%) failed to respond to bortezomib. A previous study proposed overexpression of heat-shock proteins with bortezomib resistance in lymphoma cells (14). Interleukin-6 and insulin-like growth factor may help promote cell growth and cause resistance to bortezomib (14).

It is now recognized that variable apoptotic sensitivity exists in response to bortezomib therapy, which may be due to differences in

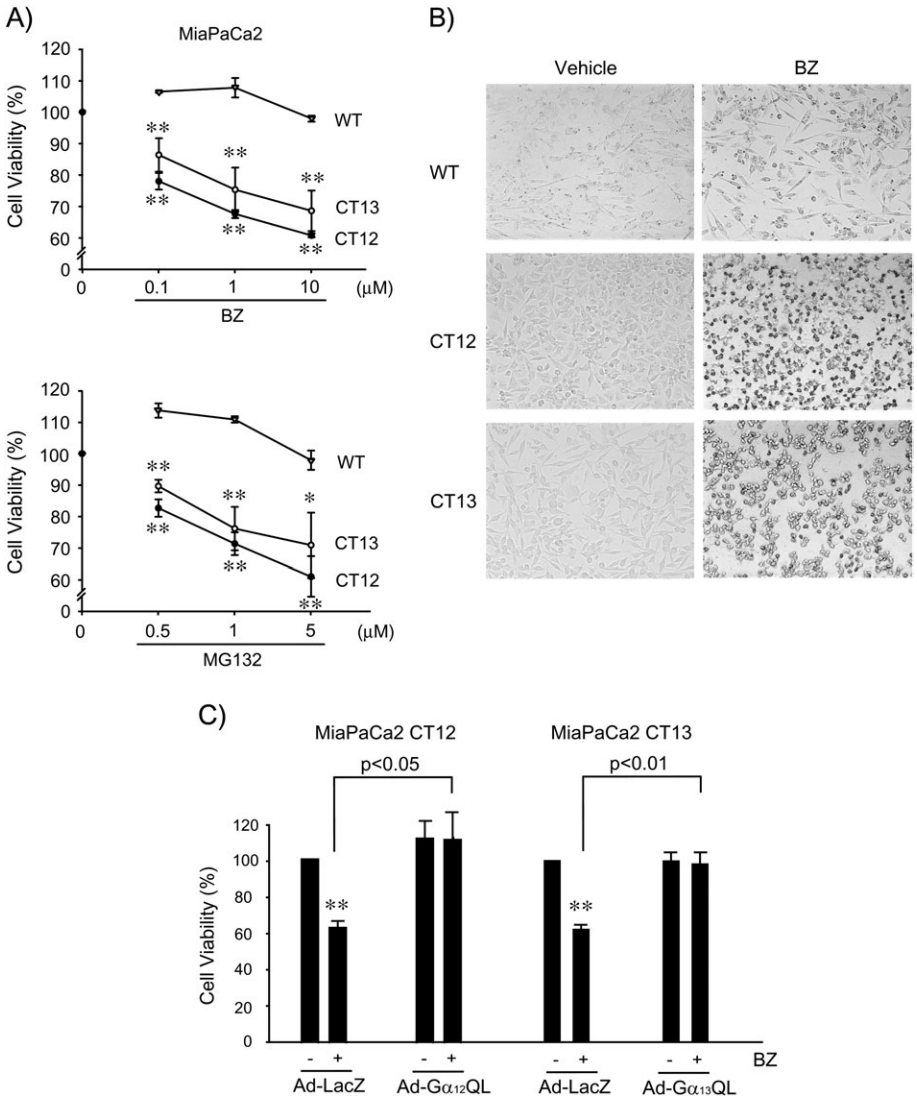

Fig. 3. The cytotoxicity of bortezomib (BZ) in MiaPaCa2 cells. (**A**) The cytotoxicity of bortezomib (0.1, 1 or 10 μM; for 24 h) or MG132 (0.5, 1 or 5 μM; for 24 h) was assessed using MTT assays in MiaPaCa2 cells that had been stably transfected with $G\alpha_{12}$ or $G\alpha_{13}$ minigene (CT12 or CT13). Data represent the mean ± SE of three independent experiments ($^{*}P < 0.05$, $^{**}P < 0.01$, significant compared with wild-type cells treated with bortezomib or MG132 at respective concentrations). (**B**) Apoptosis was monitored *in situ* using TUNEL assays in the MiaPaCa2 cells that had been treated with 10 μM bortezomib for 24 h. (**C**) The effects of $G\alpha_{12}$QL or $G\alpha_{13}$QL transfection on the cytotoxicity of bortezomib to CT12-MiaPaCa2 or CT13-MiaPaCa2 were assessed using MTT assay. Data represent the mean ± SE of three independent experiments ($^{**}P < 0.01$, significant compared with vehicle-treated control).

Table I. The relative mRNA levels of proteasome subunits in MiaPaCa2 cells or those transfected with CT12 or CT13

		Genes	Wild-type	CT12	CT13
20S proteasome	Catalytic subunit	PSMB5	1.00 ± 0.05	0.66 ± 0.08**	0.65 ± 0.10**
		PSMB6	1.00 ± 0.28	0.83 ± 0.29	0.77 ± 0.13*
		PSMB7	1.00 ± 0.21	1.58 ± 0.39	2.14 ± 0.68*
	Structural subunit	PSMA1	1.00 ± 0.33	1.68 ± 0.53	1.61 ± 0.66
		PSMA4	1.00 ± 0.15	1.04 ± 0.28	1.13 ± 0.18
		PSMC4	1.00 ± 0.11	1.57 ± 0.24*	1.59 ± 0.43
	Immunoproteasome subunit	LMP2	1.00 ± 0.12	1.06 ± 0.32	0.74 ± 0.29
		LMP7	1.00 ± 0.11	0.86 ± 0.63	0.67 ± 0.27
		MECL-1	1.00 ± 0.45	0.54 ± 0.12**	0.67 ± 0.20*
19S proteasome		RPN1	1.00 ± 0.30	1.98 ± 0.08**	1.15 ± 0.13
11S proteasome		PA28α	1.00 ± 0.07	0.29 ± 0.02**	0.40 ± 0.07**

LMP, low molecular mass polypeptide; RPN1, proteasome non-ATPase subunit 1.
Data represent the mean ± SE of three independent experiments ($^{*}P < 0.05$, $^{**}P < 0.01$, significant compared with WT MiaPaCa2 cells).

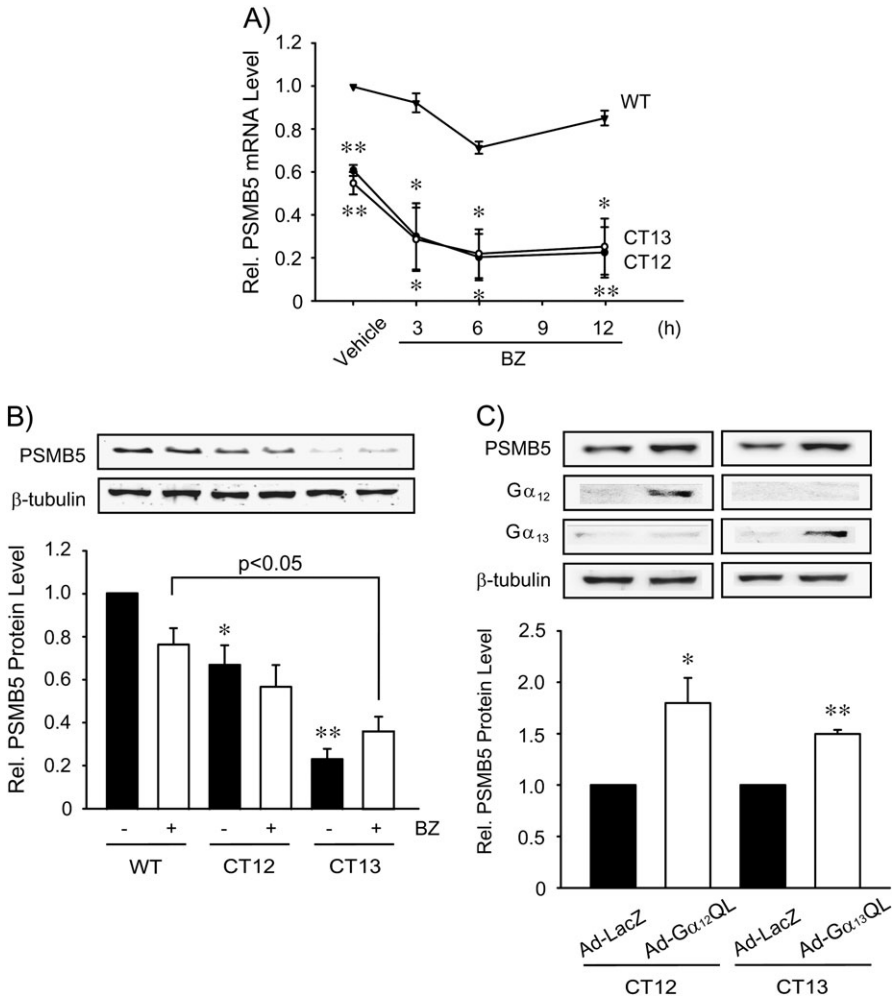

Fig. 4. Repression of PSMB5 by $G\alpha_{12}$ or $G\alpha_{13}$ minigene. (**A**) The mRNA levels of PSMB5 were measured using real-time polymerase chain reaction assay in CT12-MiaPaCa2 or CT13-MiaPaCa2 cells that had been treated with 10 μM bortezomib (BZ) for the indicated time period. The relative mRNA levels were normalized by those of hypoxanthine–guanine phosphoribosyltransferase. Results were confirmed by repeated experiments ($^{*}P < 0.05$, $^{**}P < 0.01$, significant compared with wild-type cells treated with bortezomib at respective concentrations). (**B**) The expression levels of PSMB5 protein were immunochemically monitored in the lysates of wild-type MiaPaCa2, CT12-MiaPaCa2 or CT13-MiaPaCa2 that had been treated with 10 μM bortezomib for 12 h. Immunoblottings for β-tubulin confirmed equal loading of samples. The relative levels of PSMB5 were assessed by scanning densitometry of the blots. Data represent the mean ± SE of three independent experiments ($^{*}P < 0.05$, $^{**}P < 0.01$, significant compared with untreated wild-type MiaPaCa2 cells). (**C**) The expression levels of PSMB5 were immunochemically monitored in the lysates of CT12-MiaPaCa2 or CT13-MiaPaCa2 that had been infected with Ad-LacZ, Ad-$G\alpha_{12}$QL or Ad-$G\alpha_{13}$QL (6 h). Data represent the mean ± SE of three independent experiments ($^{*}P < 0.05$, $^{**}P < 0.01$, significant compared with LacZ transfection).

the expression levels of proteasome subunits or their mutations. Importantly, several lines of evidence suggest that PSMB5 could contribute to bortezomib resistance. Study of the molecular mechanism of bortezomib resistance in human myelomonocystic cells suggested; (i) PSMB5 overexpression in resistant cells, (ii) mutation residing in a highly conserved bortezomib-binding pocket in PSMB5 and (iii) restoration of bortezomib sensitivity of resistant cells by *PSMB5* knockdown (11). The important role of PSMB5 in bortezomib resistance is supported by the increased resistance by PSMB5 overexpression (10). The G322A mutant of *PSMB5* gene conferred bortezomib resistance in Jurkat cells, causing decreased cytotoxicity, apoptosis and inhibition of chymotrypsin-like activity (12). Mutations of the *PSMB5* gene in Ala49 and Ala50 also confer varying bortezomib resistance (12).

The activated forms of $G\alpha_{12/13}$ induce a variety of biological responses including promotion of cancer cell invasion and metastasis (19,20,38): inhibition of $G\alpha_{12/13}$ signaling by the regulator of G-protein signaling homology domain of p115RhoGEF reduced the rate of metastatic dissemination of mammary carcinoma cells. Rho activation through $G\alpha_{12/13}$ may be critical for cancer invasion. Signaling via the $G\alpha_{12}$-Rho pathway may coordinate with that from cadherin to promote invasion away from the primary tumor; $G\alpha_{12/13}$ negatively regulate the adhesive function of cadherin (39). In another study, the $G\alpha_{12}$/$G\alpha_{13}$-RhoA-ROCK pathway mediates the autophosphorylation of lysophosphatidic acid-induced focal adhesion kinase and thus contributes to ovarian cancer cell migration (38). In particular, lysophosphatidic acid activates GPCRs that regulate cascades initiated by small GTPases Ras for tumor cell migration and invasion (40).

The observation that lysophosphatidic acid acyltransferase-β inhibitors induce cytotoxicity of multiple myeloma cells in patient resistant to bortezomib (41) implies that the pathways may be utilized for overcoming resistance. $G\alpha_{12}$ members serve modulators or signal transducers in diverse signaling pathways. Although $G\alpha_{12/13}$ act as modulators or signal transducers, it is yet to be elucidated whether alterations in $G\alpha_{12/13}$ expression affect the anticancer activity of bortezomib. In the present study, hepatoma cell lines displayed differential sensitivity to bortezomib in association with altered $G\alpha_{12}$ and $G\alpha_{13}$ levels, which might affect the expression of proteasome subunits and peptidase activities. Moreover, $G\alpha_{12/13}$ levels were much greater in SK-Hep1 or SNU449 cells than Huh7 or SNU886 cells, supporting

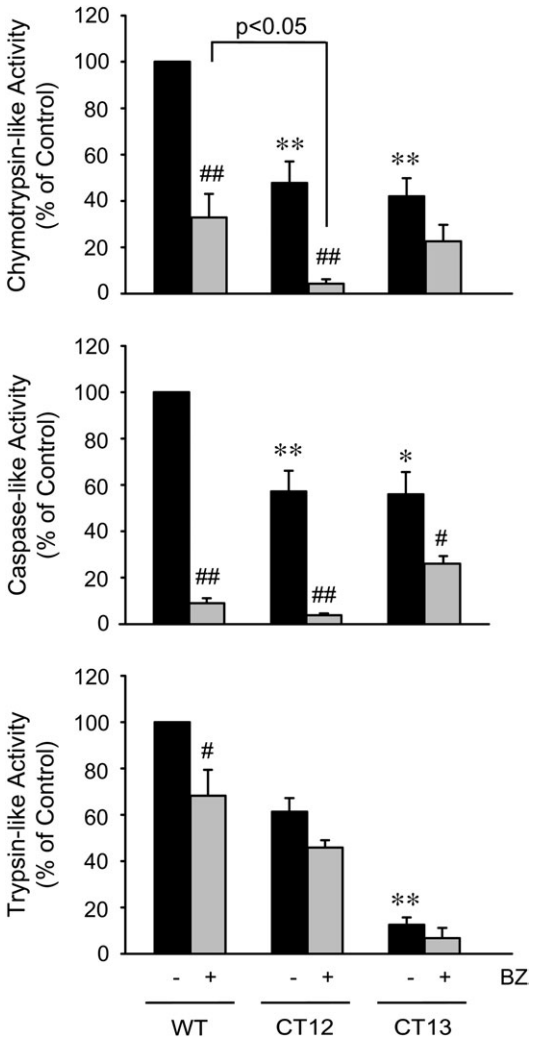

Fig. 5. Inhibition of proteasomal peptidase activities by $G\alpha_{12}$ or $G\alpha_{13}$ minigene. Chymotrypsin-like (PSMB5), caspase-like (PSMB6) and trypsin-like (PSMB7) peptidase activities were determined using *N*-Suc-LLVY-AMC, Z-LLE-AMC and Z-ARR-AMC as respective substrates in the lysates of wild-type MiaPaCa2, CT12-MiaPaCa2 or CT13-MiaPaCa2 that had been treated with 10 μM bortezomib (BZ) for 12 h. Data represent the mean ± SE of three independent experiments ($^{*}P < 0.05$, $^{**}P < 0.01$, significant compared with untreated wild-type MiaPaCa2 cells; $^{\#}P < 0.05$, $^{\#\#}P < 0.01$, significant compared with the respective MiaPaCa2 cells treated with vehicle).

the notion that high levels of $G\alpha_{12/13}$ may increase the resistance to bortezomib. This concept is strengthened by our findings that minigene inhibition of $G\alpha_{12/13}$ increased the sensitivity of mesenchymal cancer cells to bortezomib, whereas the activated mutants of $G\alpha_{12/13}$ diminished the sensitivity of epithelial cancer cells to it. Consistently, the resistant mesenchymal SK-Hep1 or SNU449 cells exhibited less sensitivity to chemotherapy than epithelial carcinoma cells.

Millennium provided the clinically relevant concentrations of bortezomib (median concentration of C_{max} is 1.3 μmol/l). In a previous study, its antitumor effect was measured in a panel of Huh7, SK-Hep1, Hep3B and PLC5. Huh7 (IC_{50} 196 nmol/l), SK-Hep1 (IC_{50} 180 nmol/l), Hep3B (IC_{50} 112 nmol/l) and PLC5 (IC_{50} >1000 nmol/l) showed reduction in cell viability after bortezomib treatment (42). In this study, SK-Hep1 cells were sensitive to bortezomib unlike ours, which may have resulted from different culture conditions. In this study, Huh7 and SK-Hep1 cells were incubated in DMEM with 5% FBS and treated with bortezomib. Our founding indicates that the levels of $G\alpha_{12/13}$ were greater in mesenchymal cells than epithelial cells after serum deprivation.

Pancreatic cancer is the fourth leading cause of cancer death in the USA. The prognosis of patients after complete resection is poor, and >50% of patients develop tumor recurrence at distant sites, with an estimated 5 year survival of 20% (43). However, the clinical response rate of standard chemotherapeutic agent (e.g. gemcitabine) is modest due to the chemoresistance in pancreatic cancer (44). MiaPaCa2 is a human pancreatic adenocarcinoma with a mesenchymal phenotype (45); in our preliminary study, we observed that $G\alpha_{12/13}$ levels were upregulated in the cell (data not shown). Moreover, MiaPaCa2 cells were extremely insensitive to bortezomib (28) and were resistant to other chemotherapeutic agents, including gemcitabine, 5-fluorouracil and cisplatin, possibly in part because of an inverse correlation between E-cadherin and its transcriptional suppressor, Zeb-1, expression (46). Our data showing increased $G\alpha_{12/13}$ expression in MiaPaCa2 cells and their enhanced sensitivity to bortezomib by minigene inhibition of $G\alpha_{12/13}$ suggest that resistance of pancreatic cancer to bortezomib (or possibly other agents) may be associated with $G\alpha_{12/13}$ expression levels.

Our result here identified PSMB5 upregulation in cells with high levels of $G\alpha_{12/13}$. The role of $G\alpha_{12/13}$ in regulating PSMB5 was strengthened by PSMB5 repression in MiaPaCa2 cells transfected with CT12 or CT13. This hypothesis is further supported by the reversal of PSMB5 repression by the reintroduction of $G\alpha_{12/13}$. These results together with the observation that $G\alpha_{12/13}$ overexpression allowed CT12- or CT13-transfected MiaPaCa2 cells to restore bortezomib resistance, verify the regulatory role of $G\alpha_{12/13}$ in proteasome function and consequent changes in bortezomib sensitivity. The notable reduction of chymotrypsin-like activity by CT12 or CT13 also supported this contention. Moreover, other proteasome subunits such as PSMB6 and PA28α were also repressed in the cells transfected with CT12 or CT13. At this time point, it has not been clearly identified as to the role of 11S complex in the function of 20S proteasome. However, a recent report showed that the 11S complex is more abundant than the 19S in HeLa cells and it is associated with 20S as well as 26S hybrid proteasome (47). This finding may account for the reduced activities in trypsin-like and caspase-like peptidases in the CT12- or CT13-transfected cells. Factors involved in the regulation of proteasome subunit expression have not been fully identified. In several reports, proteasome subunits are coordinatedly regulated, and yeast transcription factor Rpn4 and eukaryotic transcription factor Nrf2 upregulate them upon stress conditions (24,48). Since $G\alpha_{12/13}$ pathway associates with divergent cell signaling such as mitogen-activated kinases and non-receptor tyrosine kinases (49), activated $G\alpha_{12/13}$ signaling in cancer cells may affect the expression level of the proteasome system by regulating signaling components and/or transcription factors. Overall, it is highly probably that $G\alpha_{12/13}$ regulates chymotrypsin-like activity by inducing PSMB5, which may account for bortezomib resistance in mesenchymal cancer cells.

Epithelial-to-mesenchymal transition occurs in a number of diseases such as the progression of cancer (50) and is defined as the formation of mesenchymal cells from epithelia. At the molecular level, it is characterized by the loss of epithelial cell markers such as E-cadherin and the gain of mesenchymal markers. Since the disassembly of adherens junctions increases tumor cell motility and invasiveness, the acquisition of epithelial-to-mesenchymal transition features may be associated with chemoresistance, enhancing recurrence and metastasis after standard chemotherapy. In our study, $G\alpha_{12}$QL or $G\alpha_{13}$QL overexpression increased cancer aggressiveness. Moreover, morphology of Huh7 cells was also altered by $G\alpha_{12}$QL or $G\alpha_{13}$QL: epithelial-like, large, flat and spread-out appearance of the cells changed to rounded, bipolar, spindle-shaped and more fibroblastoid appearance. Likewise, the rate of cell migration was pronounced in Huh7 cells stably transfected with $G\alpha_{12}$QL or $G\alpha_{13}$QL (data not shown). These phenotypic and functional changes may be associated with the resistance of mesenchymal cancer cells to bortezomib.

In conclusion, our results demonstrate that the inhibition of $G\alpha_{12/13}$ may enhance the anticancer effect of bortezomib, and which is mediated with the repression of proteasome subunits including PSMB5, providing insight into the $G\alpha_{12/13}$ pathways for the regulation of

proteasomal activity and applications of these molecules as potential targets for cancer chemotherapy. Furthermore, targeted inhibition of $G\alpha_{12/13}$ pathway by minigene transfection may be of use to improve bortezomib therapy and reduce bortezomib resistance.

Funding

World Class University project (Ministry of Education, Science and Technology Development) (R32-2009-000-10098-0) and the National Research Foundation of Korea (MEST No. 2010-0001706) funded by the government of Korea.

Acknowledgements

Conflict of Interest Statement: None declared.

References

1. Adams,J. (2004) The proteasome: a suitable antineoplastic target. *Nat. Rev. Cancer*, **4**, 349–360.
2. Voorhees,P.M. *et al*. (2006) The proteasome and proteasome inhibitors in cancer therapy. *Annu. Rev. Pharmacol. Toxicol.*, **46**, 189–213.
3. Papandreou,C.N. *et al*. (2004) Phase I trial of the proteasome inhibitor bortezomib in patients with advanced solid tumors with observations in androgen-independent prostate cancer. *J. Clin. Oncol.*, **22**, 2108–2121.
4. Shah,M.H. *et al*. (2004) Phase II study of the proteasome inhibitor bortezomib (PS-341) in patients with metastatic neuroendocrine tumors. *Clin. Cancer Res.*, **10**, 6111–6118.
5. Davis,N.B. *et al*. (2004) Phase II trial of PS-341 in patients with renal cell cancer: a University of Chicago phase II consortium study. *J. Clin. Oncol.*, **22**, 115–119.
6. Voges,D. *et al*. (1999) The 26S proteasome: a molecular machine designed for controlled proteolysis. *Annu. Rev. Biochem.*, **68**, 1015–1068.
7. Nishiyama,A. *et al*. (2000) A nonproteolytic function of the proteasome is required for the dissociation of Cdc2 and cyclin B at the end of M phase. *Genes Dev.*, **14**, 2344–2357.
8. Tanahashi,N. *et al*. (1993) Molecular structure of 20S and 26S proteasomes. *Enzyme Protein*, **47**, 241–251.
9. Lightcap,E.S. *et al*. (2000) Proteasome inhibition measurements: clinical application. *Clin. Chem.*, **46**, 673–683.
10. Lu,S. *et al*. (2008) Overexpression of the PSMB5 gene contributes to bortezomib resistance in T-lymphoblastic lymphoma/leukemia cells derived from Jurkat line. *Exp. Hematol.*, **36**, 1278–1284.
11. Oerlemans,R. *et al*. (2008) Molecular basis of bortezomib resistance: proteasome subunit beta5 (PSMB5) gene mutation and overexpression of PSMB5 protein. *Blood*, **112**, 2489–2499.
12. Lu,S. *et al*. (2009) Different mutants of PSMB5 confer varying bortezomib resistance in T lymphoblastic lymphoma/leukemia cells derived from the Jurkat cell line. *Exp. Hematol.*, **37**, 831–837.
13. Cheriyath,V. *et al*. (2007) Proteasome inhibitors in the clinical setting: benefits and strategies to overcome multiple myeloma resistance to proteasome inhibitors. *Drugs R D*, **8**, 1–12.
14. Chauhan,D. *et al*. (2004) Targeting mitochondria to overcome conventional and bortezomib/proteasome inhibitor PS-341 resistance in multiple myeloma (MM) cells. *Blood*, **104**, 2458–2466.
15. Fields,T.A. *et al*. (1997) Signalling functions and biochemical properties of pertussis toxin-resistant G-proteins. *Biochem. J.*, **321**, 561–571.
16. Pierce,K.L. *et al*. (2002) Seven-transmembrane receptors. *Nat. Rev. Mol. Cell Biol.*, **3**, 639–650.
17. Chan,A.M. *et al*. (1993) Expression cDNA cloning of a transforming gene encoding the wild-type G alpha 12 gene product. *Mol. Cell. Biol.*, **13**, 762–768.
18. Xu,N. *et al*. (1993) A mutant alpha subunit of G12 potentiates the eicosanoid pathway and is highly oncogenic in NIH 3T3 cells. *Proc. Natl Acad. Sci. USA*, **90**, 6741–6745.
19. Kelly,P. *et al*. (2006) The G12 family of heterotrimeric G proteins promotes breast cancer invasion and metastasis. *Proc. Natl Acad. Sci. USA*, **103**, 8173–8178.
20. Kelly,P. *et al*. (2006) A role for the G12 family of heterotrimeric G proteins in prostate cancer invasion. *J. Biol. Chem.*, **281**, 26483–26490.
21. Liu,S.C. *et al*. (2009) G(alpha)12-mediated pathway promotes invasiveness of nasopharyngeal carcinoma by modulating actin cytoskeleton reorganization. *Cancer Res.*, **69**, 6122–6130.
22. Bae,E.J. *et al*. (2007) Identification of a novel class of dithiolethiones that prevent hepatic insulin resistance via the adenosine monophosphate-activated protein kinase-p70 ribosomal S6 kinase-1 pathway. *Hepatology*, **46**, 730–739.
23. Dermott,J.M. *et al*. (2002) Determining cellular role of G alpha 12. *Methods Enzymol.*, **344**, 298–309.
24. Kwak,M.K. *et al*. (2003) Antioxidants enhance mammalian proteasome expression through the Keap1-Nrf2 signaling pathway. *Mol. Cell. Biol.*, **23**, 8786–8794.
25. Fuchs,B.C. *et al*. (2008) Epithelial-to-mesenchymal transition and integrin-linked kinase mediate sensitivity to epidermal growth factor receptor inhibition in human hepatoma cells. *Cancer Res.*, **68**, 2391–2399.
26. Ki,S.H. *et al*. (2007) Galpha12 specifically regulates COX-2 induction by sphingosine 1-phosphate. Role for JNK-dependent ubiquitination and degradation of IkappaBalpha. *J. Biol. Chem.*, **282**, 1938–1947.
27. Gilchrist,A. *et al*. (2001) G alpha minigenes expressing C-terminal peptides serve as specific inhibitors of thrombin-mediated endothelial activation. *J. Biol. Chem.*, **276**, 25672–25679.
28. Nawrocki,S.T. *et al*. (2002) Effects of the proteasome inhibitor PS-341 on apoptosis and angiogenesis in orthotopic human pancreatic tumor xenografts. *Mol. Cancer Ther.*, **1**, 1243–1253.
29. Caravita,T. *et al*. (2006) Bortezomib: efficacy comparisons in solid tumors and hematologic malignancies. *Nat. Clin. Pract. Oncol.*, **3**, 374–387.
30. Llovet,J.M. *et al*. (2003) Hepatocellular carcinoma. *Lancet*, **362**, 1907–1917.
31. Burroughs,A. *et al*. (2004) Systemic treatment and liver transplantation for hepatocellular carcinoma: two ends of the therapeutic spectrum. *Lancet Oncol.*, **5**, 409–418.
32. Schwartz,M. *et al*. (2007) Strategies for the management of hepatocellular carcinoma. *Nat. Clin. Pract. Oncol.*, **4**, 424–432.
33. Shen,L. *et al*. (2008) Cell death by bortezomib-induced mitotic catastrophe in natural killer lymphoma cells. *Mol. Cancer Ther.*, **7**, 3807–3815.
34. Kamat,A.M. *et al*. (2004) The proteasome inhibitor bortezomib synergizes with gemcitabine to block the growth of human 253JB-V bladder tumors in vivo. *Mol. Cancer Ther.*, **3**, 279–290.
35. Chesnel,F. *et al*. (2006) Cyclin B dissociation from CDK1 precedes its degradation upon MPF inactivation in mitotic extracts of *Xenopus laevis* embryos. *Cell Cycle*, **5**, 1687–1698.
36. Lee,S.J. *et al*. (2008) Bortezomib is associated with better health-related quality of life than high-dose dexamethasone in patients with relapsed multiple myeloma: results from the APEX study. *Br. J. Haematol.*, **143**, 511–519.
37. Richardson,P.G. *et al*. (2003) A phase 2 study of bortezomib in relapsed, refractory myeloma. *N. Engl. J. Med.*, **348**, 2609–2617.
38. Bian,D. *et al*. (2006) The G12/13-RhoA signaling pathway contributes to efficient lysophosphatidic acid-stimulated cell migration. *Oncogene*, **25**, 2234–2244.
39. Meigs,T.E. *et al*. (2002) Galpha12 and Galpha13 negatively regulate the adhesive functions of cadherin. *J. Biol. Chem.*, **277**, 24594–24600.
40. Mills,G.B. *et al*. (2003) The emerging role of lysophosphatidic acid in cancer. *Nat. Rev. Cancer*, **3**, 582–591.
41. Hideshima,T. *et al*. (2005) Molecular characterization of PS-341 (bortezomib) resistance: implications for overcoming resistance using lysophosphatidic acid acyltransferase (LPAAT)-beta inhibitors. *Oncogene*, **24**, 3121–3129.
42. Chen,K.F. *et al*. (2008) Down-regulation of phospho-Akt is a major molecular determinant of bortezomib-induced apoptosis in hepatocellular carcinoma cells. *Cancer Res.*, **68**, 6698–6707.
43. Li,D. *et al*. (2004) Pancreatic cancer. *Lancet*, **363**, 1049–1057.
44. Oettle,H. *et al*. (2007) Adjuvant chemotherapy with gemcitabine vs observation in patients undergoing curative-intent resection of pancreatic cancer: a randomized controlled trial. *JAMA*, **297**, 267–277.
45. Barbera,M.J. *et al*. (2004) Regulation of Snail transcription during epithelial to mesenchymal transition of tumor cells. *Oncogene*, **23**, 7345–7354.
46. Arumugam,T. *et al*. (2009) Epithelial to mesenchymal transition contributes to drug resistance in pancreatic cancer. *Cancer Res.*, **69**, 5820–5828.
47. Tanahashi,N. *et al*. (2000) Hybrid proteasomes. Induction by interferon-gamma and contribution to ATP-dependent proteolysis. *J. Biol. Chem.*, **275**, 14336–14345.
48. Xie,Y. *et al*. (2001) RPN4 is a ligand, substrate, and transcriptional regulator of the 26S proteasome: a negative feedback circuit. *Proc. Natl Acad. Sci. USA*, **98**, 3056–3061.
49. Kelly,P. *et al*. (2007) Biologic functions of the G12 subfamily of heterotrimeric g proteins: growth, migration, and metastasis. *Biochemistry*, **46**, 6677–6687.
50. Huber,M.A. *et al*. (2005) Molecular requirements for epithelial-mesenchymal transition during tumor progression. *Curr. Opin. Cell Biol.*, **17**, 548–558.

Received March 27, 2010; revised May 7, 2010; accepted May 10, 2010